Proc. Natl. Acad. Sci. USA
Vol. 87, pp. 7888–7892, October 1990
Biophysics

Effect of specific mutations of tyrosine-(M)210 on the primary photosynthetic electron-transfer process in *Rhodobacter sphaeroides*

(bacterial photosynthesis/reaction centers/site-directed mutagenesis/picosecond kinetics/spectral relaxation)

V. NAGARAJAN†, W. W. PARSON†, D. GAUL‡, AND C. SCHENCK‡

†Department of Biochemistry, SJ-70, University of Washington, Seattle, WA 98195; and ‡Department of Biochemistry, Colorado State University, Fort Collins, CO 80523

Communicated by R. A. Marcus, July 13, 1990

ABSTRACT **We have measured the rate of the initial electron-transfer process as a function of temperature in reaction centers in a native strain of the photosynthetic bacterium *Rhodobacter sphaeroides* and two mutants generated by site-directed mutagenesis. In the mutants, a tyrosine residue in the vicinity of the primary electron donor and acceptor molecules was replaced by either phenylalanine or isoleucine. The electron-transfer reaction is slower in the mutants and has a qualitatively different dependence on temperature. In native reaction centers the rate increases as the temperature is reduced, in the phenylalanine mutant it is virtually independent of temperature, and in the isoleucine mutant it decreases with decreasing temperature. At 77 K, the electron-transfer reaction is ≈30 times slower in the isoleucine mutant than in the native. These observations support the view that tyrosine-(M)210 plays an important role in the electron-transfer mechanism. In the isoleucine mutant at low temperatures, the stimulated emission from the excited reaction center undergoes a time-dependent shift to shorter wavelengths.**

In purple photosynthetic bacteria, light initiates a series of electron-transfer reactions in a pigment–protein complex known as the reaction center (RC). X-ray crystallographic studies have shown that the pigments of the RC are arranged symmetrically on two protein subunits, L and M (1–3). Light absorption excites a bacteriochlorophyll dimer designated as P. Near P are two "accessory" bacteriochlorophylls (B_L and B_M), two bacteriopheophytins (H_L and H_M), and two quinones. The excited dimer (P*) transfers an electron to H_L in ≈3 ps (4–6). Why excitation reduces only one of the two bacteriopheophytins is not yet clear (7, 8). Moreover, no consensus exists on the function of the accessory bacteriochlorophylls. Although B_L is located between P and H_L, several ultrafast spectroscopic studies (4, 5, 9) have given no indication that a $P^+B_L^-$ radical pair forms as an intermediate in the electron-transfer reaction. One recent study, however, offers evidence for such an intermediate (6).

Although the L and M subunits have similar primary and secondary structures, they also have several notable differences. In the crystal structures of *Rhodobacter sphaeroides* and *Rhodopseudomonas viridis* RCs, a tyrosine residue [(M)Y210 in *Rb. sphaeroides*, (M)Y208 in *Rp. viridis*] is close to P, B_L, and H_L (Fig. 1) (1–3). The corresponding residue on the opposite side is phenylalanine. Calculations based on the *Rp. viridis* structure suggest that electrostatic interactions with the tyrosine lower the energy of the state $P^+B_L^-$, thus aiding electron transfer along the L side (10). In the RCs of the thermophilic bacterial species *Chloroflexus aurantiacus*, this tyrosine residue is replaced by leucine, which may explain the slower electron-transfer kinetics observed there (11). Moreover, the aromatic ring of the tyrosine could act as a conduit for an electron, as has been suggested for electron-transfer processes in some heme proteins. These considerations lead naturally to employing site-directed mutagenesis to explore the factors that determine direction and rate of the initial electron-transfer reaction. Using picosecond absorption spectroscopy, we have measured the electron-transfer kinetics in RCs of native bacteria and of mutants in which tyrosine-(M)210 is replaced by phenylalanine-[(M)Y210F] or isoleucine-[(M)Y210I]. Because raising the energy of $P^+B_L^-$ might be expected to alter the temperature dependence of the electron-transfer reaction, we also studied how the kinetics vary with temperature in the three RCs. Mutants with phenylalanine or leucine at position (M)210 also have been prepared recently by Gray *et al.* (12).

EXPERIMENTAL PROCEDURES

Oligonucleotide site-directed mutations were constructed by the phosphorothioate selection method (13). A 1.3-kilobase (kb) *Sal* I–*Hin*d III DNA restriction fragment carrying the M gene of the bacterial *puf* operon (14) was ligated into M13 mp19 phage. Synthetic oligonucleotides encoding variants in the (M)210 codon were hybridized to the single-stranded DNA, and a covalently closed heteroduplex DNA molecule was created by *in vitro* recombinant techniques (15). The heteroduplexes were transfected into an *Escherichia coli* host, and the resultant phage plaques were screened for the presence of the desired mutation and absence of secondary mutations by dideoxynucleotide sequencing (16). Mutant DNA fragments were recombined with the wild-type 5′ end of the *puf* operon and placed in a broad host-range expression vector (17), which was crossed into a *puf*-deletion background of *Rb. sphaeroides* (18). Exconjugants were selected on tetracycline (3 μg/ml), purified, and tested for photosynthetic growth. Mass cultures were grown in the dark at 34°C in 4-liter Erlenmeyer flasks filled to 80% capacity.

RCs from *Rb. sphaeroides* R-26 (a carotenoidless strain), the wild-type strain WS231, and the mutants were purified essentially as described for R-26 (4). The absorbance ratios A_{280} nm/A_{800} nm were typically between 1.1 and 1.2. Several different samples of RCs from each mutant strain, including samples purified further by HPLC, displayed the same kinetics within experimental uncertainty. In experiments at room temperature, RC samples in 10 mM Tris·HCl/0.1% lauryldimethylamine oxide (vol/vol)/10 mM EDTA, pH 8.0, were passed through a 1-mm-path-length cuvette from a reservoir kept in an ice bath. Absorbance at 800 nm was usually between 1.3 and 1.4 per mm. For lower temperatures, the samples also contained 60% (vol/vol) glycerol and were housed in a Dewar (Kontes 611770) that was cooled by cold N_2 gas; these samples were not circulated. Films of R-26 RCs in poly(vinyl alcohol) also were used at low temperatures.

The publication costs of this article were defrayed in part by page charge payment. This article must therefore be hereby marked "*advertisement*" in accordance with 18 U.S.C. §1734 solely to indicate this fact.

Abbreviation: RC, reaction center.

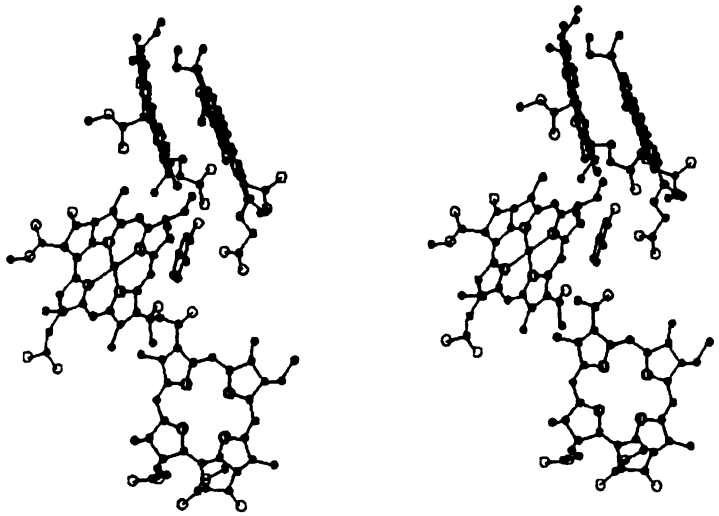

FIG. 1. Stereo view showing the side chain of tyrosine-(M)210 in relation to the pigments in *Rb. sphaeroides* R-26 reaction centers. The bacteriochlorophyll dimer (P) is at top, H_L is at bottom, and B_L is in the middle on left; B_M and H_M are not shown. ○, Oxygen atoms; ●, carbons. The x-ray coordinates (2) were provided by J. Allen, D. Rees, and G. Feher (University of California, San Diego).

The picosecond spectrometer was as described (4), except that, after passing through the sample, the two probe beams were focused on the entrance slits of separate 0.25-m monochromators to disperse them onto linear diode arrays of 512 elements [Hamamatsu (Tokyo) type 2301-512Q]. This setup provided a 350-nm absorption spectrum on each laser flash. Good signal-to-noise ratios were achieved by averaging between 100 and 500 flashes. Background traces collected with the picosecond light blocked were subtracted from each raw spectrum before calculating difference spectra.

Kinetic data were fit by nonlinear least-squares analysis to a convolution of an "instrument" function and a theoretical function, with a wavelength-dependent time shift that was treated as an additional free parameter. The instrument function was generated by taking the first derivative of the signal at ≈850 nm (4). The stimulated-emission signals from R-26 or WS231 RCs were fit well with a single-exponential decay plus a constant. With the (M)Y210I RCs, single-exponential fits to data at low temperatures were unacceptable as judged by the residuals. Biexponential fits also were unsatisfactory because the time constants were not reproducible among different sets of data and were poorly correlated with temperature or wavelength. A more suitable treatment was obtained by using the function $A \exp\{-(k_0 t)^\alpha\} + B$, where A, k_0, α, and B are constants and $0 < \alpha \leq 1$. The "stretched-exponential" function $\exp\{-(k_0 t)^\alpha\}$ has been used to describe the decay of transient species in glassy media (19). If the stretched-exponential function is equated to a continuous distribution of single-exponential terms, $\int_0^\infty f(k) e^{-kt} dk$, the mean time constant is given by $\langle\tau\rangle = (1/\alpha k_0)\Gamma(1/\alpha)$, where Γ is the gamma function (19). For a single-exponential decay $\alpha = 1$ and $\langle\tau\rangle$ reduces to $1/k_0$. The curve-fitting procedure was tested by fitting synthetic data that included random noise. The correct time constant always was recovered (within ±10%) with a usual spread in the value of α of ±0.1 about 1.0, but the spread in α could be as much as ±0.2 if the peak signal-to-noise ratio was ≤3. Because the signal-to-noise ratio in the experimental data generally was greater than 3, a systematic deviation of α from 1.0 is diagnostic of nonexponential kinetics.

RESULTS

The spectral changes in the 700- to 950-nm region are very similar in RCs of the native and mutant bacteria (Fig. 2). The isobestic point near 800 nm is consistent with a transformation involving only two resolvable states, P* and $P^+H_L^-$. [The excitation pulses that we used were not well suited for resolving the additional transient that Holzapfel *et al.* (6) have interpreted as $P^+B_L^-$; the pulses were somewhat too long and were at a wavelength (605 nm) that would excite B_L and B_M in addition to P.] The instantaneous formation of the stimulated-emission band is seen as a shoulder on the long-wavelength side of the bleaching in the 870-nm region. After decay of the stimulated emission, there remains a Gaussian-shaped bleaching of the 870-nm band. In all strains, this band sharpens and shifts to longer wavelengths with decreasing temperature, as described for native RCs (20). At 77 K, the bleaching is centered at 890 nm. As stimulated emission decays, the signal at 760 nm evolves from an absorbance increase associated with P* to the bleaching that reflects reduction of H_L.

Stimulated-emission spectra can be obtained by subtracting the difference spectrum measured at long times (three to five lifetimes) from spectra measured at earlier times, after normalization to correct for changes in P* concentration (4). We used the region on the short-wavelength side of the 870-nm band for the normalization on the assumption that the bleaching here contains no significant contribution from stimulated emission. At a given temperature, the shapes of the normalized emission spectra were very similar for the native and mutant RCs. With each strain, the spectrum narrowed and shifted to longer wavelengths as the temperature was lowered. The emission maximum moved from ≈915 nm at 295 K to 935 nm at 77 K.

To determine the peak positions and width of the stimulated-emission spectra quantitatively, we fit the spectra to a log-normal function (21). In the native and (M)Y210F RCs, the peak position and width were essentially invariant in time up to at least one lifetime. This result indicates that the

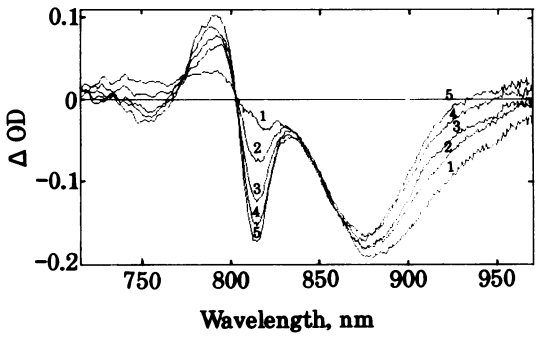

FIG. 2. Absorbance changes after excitation of (M)Y210F RCs at room temperature. Spectra 1–5 correspond to time delays of 1, 6, 11, 21, and 51 ps relative to excitation. Each spectrum is the average of 100 flashes.

electron transfer probably ensues from a vibrationally equilibrated state of P*, in agreement with the results from transient hole-burning experiments (22). In the (M)Y210I RCs, no change in the peak position or shape could be resolved at room temperature (Fig. 3, *Upper right*), but at 77 K the emission maximum shifted by ≈3.5 nm to shorter wavelengths during the first few picoseconds (Fig. 3, *Upper left*). The bandwidth appeared not to change. Plotting the deviation from the final peak frequency as a function of time and assuming an exponential time dependence gave a time constant of 3.0 ± 1.5 ps for the shift. The amplitude spectra derived by fitting the decay kinetics of the stimulated emission at various wavelengths across the band shift similarly (Fig. 3, *Lower left*). (These latter spectra take into account the wavelength-dependent time shift between the excitation and probe pulses.)

At room temperature, the initial electron-transfer reaction in native (R-26 and WS231) RCs was found to proceed with a time constant (τ_{IET}) of 3.5 ± 0.3 ps; this result agrees well with several reports (4, 6, 23) but is somewhat longer than the time constant of 2.8 ps reported by Martin and coworkers (5, 24). The decay of stimulated emission in the 915-nm region and the development of the bleaching in the 760-nm region both were well fit to single-exponential decays with the same τ_{IET} within experimental error. As temperature was lowered, the rate constant k_{IET} ($=1/\tau_{IET}$) increased in both of these strains (Fig. 4 *Top*), as has been found before with R-26 (4, 24). In contrast to an earlier report that the decay of P* at 77 K was faster in 60% glycerol than in a poly(vinyl alcohol) film (4), we found that the temperature dependence of k_{IET} in the two types of samples was essentially the same.

When tyrosine (M)210 is replaced by phenylalanine, τ_{IET} increases ≈3-fold to 10.5 ± 1.0 ps at room temperature. In the (M)Y210I RCs, τ_{IET} is increased further to 16 ± 1 ps. With mutant RCs, the time constant from a single-exponential fit to data at 760 nm at room temperature was ≈50% shorter than that obtained from the stimulated emission. This discrepancy is explainable on the basis of partial reoxidation of H_L^- during the experimental time window due to electron transfer to the next acceptor, quinone Q_A (25). No attempt was made to extract the time constant for this additional step. Therefore, the rate constants reported for (M)Y210F and (M)Y210I come solely from the measurements of stimulated emission.

With both mutants, as in the native RCs, fits of room-temperature data to the stretched-exponential function gave $\alpha \approx 1$, with no systematic dependence on wavelength. When the mutant RCs were cooled below 190 K, data obtained on the long-wavelength side of the emission band required values of $\alpha < 1$ for best fit. Examples of fits to data on (M)Y210I RCs at various temperatures are shown in Fig. 5; with this mutant, α and $\langle\tau\rangle$ both decreased systematically with increased wavelength. At 135 K, for example, the values of α and $\langle\tau\rangle$ were 0.82 and 54 ps at 925 nm and 0.72 and 38 ps at 950 nm. As mentioned under *Experimental Procedures*,

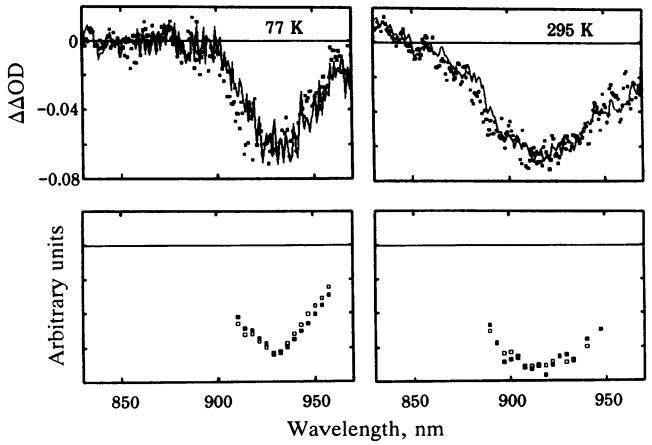

FIG. 3. (*Upper*) Normalized spectra of stimulated emission from (M)Y210I RCs at 1 ps (line) and 11 ps (squares) after excitation at 77 K and at 0 ps (line) and 10 ps (squares) at 295 K. (*Lower*) Normalized amplitude spectra from stretched-exponential fits of the kinetics at each wavelength, calculated for 1 ps (■) and 11 ps (□) after excitation at 77 K and for 0 ps (■) and 10 ps (□) at 295 K.

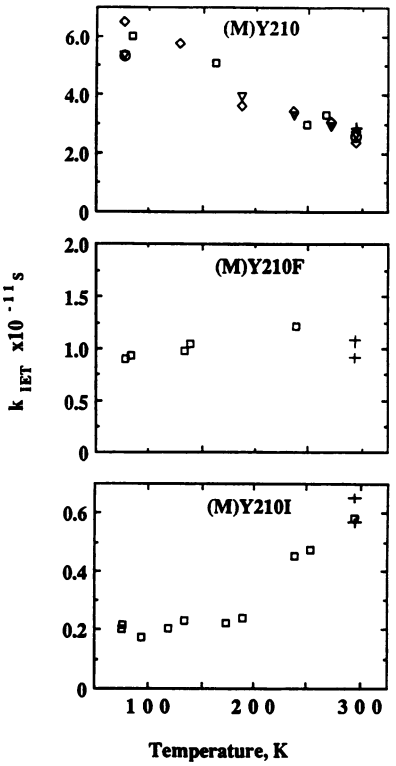

FIG. 4. Temperature-dependence of the electron-transfer rate constants in native and mutant RCs. (*Top*, *Middle*, *Bottom*) $k_{IET} = 1/\langle\tau\rangle$, measured near the peak in the emission spectrum; +, RCs in aqueous detergent/buffer; □, RCs in 60% (vol/vol) glycerol. (*Top*) ○, WS231 RCs in glycerol; ◇ and ▽, different R-26 in poly(vinyl alcohol) films.

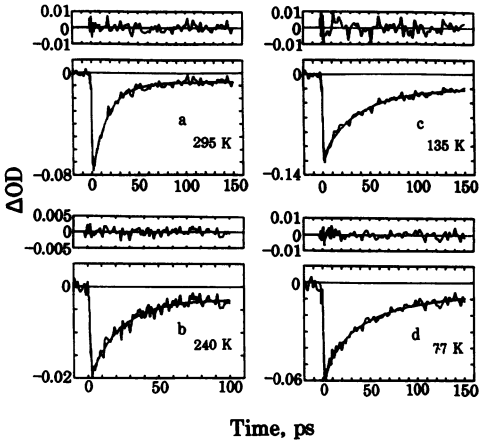

FIG. 5. Kinetics of stimulated emission from (M)Y210I RCs at 295, 240, 135, and 77 K, measured at 915 nm (*a* and *b*) or 935 nm (*c* and *d*) with a 5-nm bandwidth. The smooth curves are fits to the stretched-exponential function with the following values for α and $\langle\tau\rangle$: (*a*) 0.95 and 17.4 ps; (*b*) 1.0 and 21.7 ps; (*c*) 0.74 and 42.6 ps; and (*d*) 0.67 and 47.6 ps. The upper spectrum corresponding to each curve shows the difference between the fitted function and the experimental data, expressed in OD units.

the addition of random noise to synthetic exponential decay data made α depart from 1.0. However, this effect was significant only when the signal-to-noise ratio was relatively low; the experimentally determined values of α were consistently <1, regardless of signal-to-noise ratio. For (M)Y210I, departure of α from 1.0 and the wavelength-dependence of α and $\langle\tau\rangle$ can be attributed partly to the time-dependent shift in the emission spectrum. In (M)Y210F RCs, where a spectral shift was not resolvable, $\langle\tau\rangle$ was virtually unchanged across the emission band, but α again was <1.

The most dramatic difference between the wild-type and mutant RCs is in the temperature dependence of k_{IET} (Fig. 4). In (M)Y210F, k_{IET} is independent of temperature. In (M)-Y210I, k_{IET} *decreases* with decreasing temperature down to 190 K but then becomes temperature-independent. For the mutant RCs, k_{IET} was calculated near the peak of the stimulated-emission band, where any effects of spectral shifting should be small, but the general form of the temperature dependence of k_{IET} is preserved over a large wavelength range. At 80 K the rate constants in the wild type and (M)Y210I RCs differ by a factor of ≈30.

DISCUSSION

Replacing tyrosine-(M)210 by phenylalanine or isoleucine significantly affects the initial electron-transfer step. Three observations need explanation: the decrease in k_{IET} as we move from native RCs to (M)Y210F to (M)Y210I at a fixed temperature, the qualitatively different temperature dependences of k_{IET} in the three types of RC, and the nonexponential kinetics seen with the mutant RCs at low temperatures. K. Gray and W. Zinth (personal communication) have made measurements similar to ours on phenylalanine and leucine mutants at room temperature. They also found increased time constants in the two mutants (16 ± 4 ps with phenylalanine and 22 ± 8 with leucine).

The phenolic OH group of tyrosine-(M)210 can interact electrostatically with the pigments in its vicinity (10, 26), while the phenyl ring could possibly provide a pathway for the electron from P* to H_L. If electrostatic interactions involving the OH group are the most critical in determining electron-transfer rate, one might expect similar changes in rate when the tyrosine is replaced by either phenylalanine or isoleucine. On the other hand, if the tyrosine acts as a conduit for the electron, then substitution by phenylalanine might be predicted to have much less effect on rate than substitution by isoleucine. Neither of these limiting hypotheses is fully consistent with experimental results. The rate constant measured at 295 K decreased ≈3-fold when tyrosine was replaced by phenylalanine and ≈5-fold with isoleucine. This result suggests that electrostatic interactions with the phenolic group and electron conduction both could be important factors in determining the rate. But this analysis presupposes that the mutations modify the side chain of residue (M)210 without causing any rearrangement of consequence of the surrounding structure, which may not be the case. Because the isoleucine side chain is less rigid and somewhat smaller than those of tyrosine and phenylalanine, this side chain could cause a greater rearrangement of the local protein structure, thus influencing the electron-transfer rate in ways difficult to predict. Free-energy-perturbation calculations, in which the structure is allowed to relax in response to the mutation, indicate that (*i*) replacing tyrosine-(M)208 in the *Rp. viridis* structure by phenylalanine probably causes a somewhat smaller increase in the energy of $P^+B_L^-$ than one expects from the static crystal structure and (*ii*) mutation to isoleucine would result in a greater increase in the energy (26).

The observation that the initial electron-transfer reaction in native RCs increases in speed with decreasing temperature has been explained by postulating that the potential-energy curve of the product state crosses the curve for the reactant near the latter's minimum (27–30). (For an alternative view, see ref. 23.) If intersection of the potential-energy curves occurs well above the minimum of the reactant curve, the reaction will require thermal activation. For an intermediate value of the barrier energy E_b (measured from bottom of the reactant curve), the reaction will be temperature-independent (30). Even when E_b is large, however, the rate can become temperature-independent at low temperatures when nuclear tunneling dominates. If the initial product state is $P^+B_L^-$ (6, 10, 31), our results can be explained simply by assuming that the mutations raise the energy of $P^+B_L^-$ so that $0 \approx E_b(WS231) < E_b[(M)Y210F] < E_b[(M)Y210I]$. In this model the initial electron-transfer reaction in the (M)Y210I RCs is thermally activated near room temperature, but the activated process becomes so slow at temperatures below 190 K that tunneling takes over. The (M)Y210F RCs would fall in the intermediate region where k_{IET} neither decreases nor increases with temperature.

We can obtain an estimate of E_b in (M)Y210I RCs from the activation energy for electron transfer at high temperatures (Fig. 4 *Bottom*). After subtracting the low-temperature (tunneling) rate constant from the data between 240 K and 295 K, the apparent activation energy is 1.30 kcal/mol (1 cal = 4.184 J). Another way of estimating E_b is to assume that the τ_{IET} of ≈2 ps in R-26 RCs at 77 K reflects the limiting Franck–Condon factor of 1 for $E_b = 0$ and that the mutations do not alter the electronic coupling strength between the reactant and product states. From the electron-transfer time constant of 16 ps in (M)Y210I RCs at room temperature, these assumptions lead to $E_b \approx 1.25$ kcal/mol, which is close to the value obtained above. Similarly, $\tau_{IET} \approx 10$ ps at room temperature leads to $E_b \approx 0.95$ kcal/mol for (M)Y210F RCs. These values appear qualitatively in accord with the free-energy-perturbation calculations based on *Rp. viridis* crystal structure (26). Comparable electrostatic calculations have not yet been performed on the *Rb. sphaeroides* crystal structures (2, 3), which are still undergoing refinement.

An alternative explanation for our results could be given in terms of the superexchange mechanism of electron transfer (4, 31–33). In this mechanism, the function of B_L or the protein is to couple the reactant and product states electronically. The coupling strength will vary as the inverse of the energy (E_{int}) of the virtual intermediate state (for example, $P^+B_L^-$), measured from the point of intersection of the potential energy curves of P* and $P^+H_L^-$. If the mutations increase E_{int} so that $E_{int}(WS231) < E_{int}[(M)Y210F] < E_{int}[(M)Y210I]$, then at a given temperature k_{IET} would decrease going from left to right. Because temperature dependence of k_{IET} would hinge primarily on the energy of the intersection point between P* and $P^+H_L^-$, the superexchange mechanism would require that the mutations also raise the energy of $P^+H_L^-$ relative to P*. However, the phenolic group of tyrosine-(M)210 is farther from H_L than it is from B_L (Fig. 1), and electrostatics calculations on the *Rp. viridis* structure suggest that replacing the tyrosine by phenylalanine would have less effect on the energy of $P^+H_L^-$ than on the energy of $P^+B_L^-$ (10). The temperature dependence of k_{IET} also could reflect thermal expansion of the protein and consequent changes in the electronic coupling of P, B_L, and H_L.

The nonexponential reaction kinetics seen in the mutant RCs at low temperatures could result partly from conformational heterogeneity. Such heterogeneity might occur in the mutants, where a tyrosine is replaced by a residue that is somewhat smaller and that lacks the stabilizing influence of the rigid aromatic ring or the phenolic OH group. Its effects might be most evident at low temperatures, where interconversions among different conformational states would occur relatively slowly. Conformational heterogeneity also could

account for the shifting of the stimulated-emission spectrum to shorter wavelengths in the (M)Y210I RCs during the first few picoseconds after excitation. If RC molecules with conformations favorable for charge separation corresponded to the long-wavelength side of the emission spectrum, then that side of the band would decay faster than the short-wavelength side, leading to an apparent shift of the emission spectrum. However, comparison of the absorption-band shapes of the native and mutant RCs at 77 K reveals no evidence of enhanced spectral heterogeneity. That width of the normalized emission spectrum remains constant also is more consistent with a true shift of the emission than with a selective depletion of components on the long-wavelength side.

It is unclear whether the blue-shift seen with the mutant RCs reflects a process relevant to the electron-transfer kinetics, such as the vibrational relaxation of P*. Spectral shifts of excited molecules in solution often result from reorientation of polar solvent molecules but usually proceed in the direction of lower energies. The stimulated emission from monomeric bacteriochlorophyll in propanol, for example, shifts ≈10 nm to longer wavelengths after excitation (34). However, in a multidimensional system, the energy of a mode coupled to the optical transition could increase, while the excited system as a whole relaxes. In our experiments, the shift was obvious only in the (M)Y210I mutant at low temperatures, but this result could be simply because the relatively long lifetime of P* in this strain provides a wide experimental window for the measurements. Sharpening of the emission band at low temperatures also would make it easier to resolve the shift. However, as just mentioned, the smaller and more flexible side chain of isoleucine may also allow the RC to undergo larger changes in conformation after excitation.

The long lifetime of P* in the mutant RCs puts an upper limit on the rate of nonradiative decay of P* to ground state. Fig. 2 shows that for (M)Y210F RCs at room temperature, bleaching on the short-wavelength side of the 870-nm band does not reverse significantly during the lifetime of P*. Similar results were obtained for all three strains at all temperatures. Because a reversal of 5% of bleaching probably could have been resolved, the time constant for decay to ground state appears at least 20-fold greater than the measured lifetime of P*. The decay time in (M)Y210I, therefore, must be at least 0.3 ns at 295 K and at least 1 ns at low temperatures. Because a charge-transfer state mixed in with P* can couple the ground and excited states of P electronically (33), the slow decay probably reflects the poor Franck–Condon overlap resulting from the large energy gap (33 kcal/mol) between the two states.

We thank G. Feher for the R-26/poly(vinyl alcohol) films, A. Warshel and M. Becker for helpful discussions, D. Middendorf for help with the instrumentation, M. Larvie for technical help, and K. Gray and W. Zinth for informing us of their unpublished results. This work was supported by National Science Foundation Grant PCM-8616161 to W.W.P. and by grants from the United States Department of Agriculture-Competitive Research Grants Office (87-CRCR-1-2358), National Institutes of Health (R26GM-38214 and K04GM-00536), and the Colorado Agricultural Research Station to C.S. D.G. is a National Science Foundation Plant Biology Postdoctoral Fellow.

1. Michel, H., Epp, O. & Deisenhofer, J. (1986) *EMBO J.* **5,** 2445–2451.
2. Yeates, T. O., Komiya, H., Chirino, A., Rees, D. C., Allen, J. P. & Feher, G. (1988) *Proc. Natl. Acad. Sci. USA* **85,** 7993–7997.
3. Tiede, D. M., Budil, D. E., Tang, J., El Kabbani, O., Norris, J. R., Chang, C. H. & Schiffer, M. (1988) in *The Photosynthetic Bacterial Reaction Center*, eds. Breton, J. & Vermeglio, A. (Plenum, New York), pp. 13–20.
4. Woodbury, N. W., Becker, M., Middendorf, D. & Parson, W. W. (1985) *Biochemistry* **24,** 7516–7521.
5. Martin, J. L., Breton, J., Lambry, J. C. & Fleming, G. (1988) in *The Photosynthetic Bacterial Reaction Center*, eds. Breton, J. & Vermeglio, A. (Plenum, New York), pp. 195–203.
6. Holzapfel, W., Finkele, U., Kaiser, W., Oesterhelt, O., Sheer, H., Stilz, H. U. & Zinth, W. (1989) *Chem. Phys. Lett.* **160,** 1–7.
7. Knapp, E. W., Fischer, S. F., Zinth, W., Sander, M., Kaiser, W., Deisenhofer, J. & Michel, H. (1985) *Proc. Natl. Acad. Sci. USA* **82,** 8463–8467.
8. Bylina, E. J., Kirmaier, C., McDowell, L., Holten, D. & Youvan, D. C. (1988) *Nature (London)* **336,** 182–184.
9. Kirmaier, C. & Holten, D. (1988) *FEBS Lett.* **239,** 211–218.
10. Parson, W. W., Chu, Z.-T. & Warshel, A. (1990) *Biochim. Biophys. Acta* **1017,** 251–272.
11. Becker, M., Middendorf, D., Woodbury, N. W., Parson, W. & Blankenship, R. E. (1986) in *Ultrafast Phenomena V*, eds. Fleming, G. R. & Siegman, A. E. (Springer, New York), pp. 374–378.
12. Gray, K. A., Farchaus, J. W., Wachtveitl, J., Breton, J. & Oesterhelt, D. (1990) *EMBO J.* **9,** 2061–2070.
13. Taylor, J. W., Ott, J. & Eckstein, F. (1985) *Nucleic Acids Res.* **13,** 8764–8785.
14. Williams, J. C., Steiner, L. A., Feher, G. & Simon, M. I. (1984) *Proc. Natl. Acad. Sci. USA* **81,** 7303–7308.
15. Maniatis, T., Fritsch, E. F. & Sambrook, J. (1982) *Molecular Cloning: A Laboratory Manual* (Cold Spring Harbor Lab., Cold Spring Harbor, NY).
16. Sanger, F., Nicklen, S. & Coulson, A. R. (1977) *Proc. Natl. Acad. Sci. USA* **74,** 5463–5468.
17. Keen, N. T., Tamaki, S., Kobayashi, D. & Trollinger, D. (1988) *Gene* **70,** 191–197.
18. Gaul, D., Brasher, B., Martin, K. & Schenck, C. (1989) *Biophys. J.* **55,** 181 (abstr.).
19. Plonka, A. (1988) in *Time Dependent Reactivity of Species in Condensed Media*, Lecture Notes in Chemistry, eds. Berthier, G., Dewar, M. J. S., Fischer, H., Fukui, K., Hall, G. G., Hartmann, H., Jaffé, H. H., Jortner, J., Kutzelnigg, W., Ruedenberg, K. & Tomasi, J. (Springer, Berlin), Vol. 40, p. 151.
20. Kirmaier, C. & Holten, D. (1988) in *The Photosynthetic Bacterial Reaction Center*, eds. Breton, J. & Vermeglio, A. (Plenum, New York), pp. 219–228.
21. Nagarajan, V., Brearley, A. M., Kang, T. J. & Barbara, P. F. (1987) *J. Chem. Phys.* **86,** 3183–3187.
22. Johnson, S. G., Tang, D., Jankowiak, R., Hayes, J. M., Small, G. J. & Tiede, D. M. (1989) *J. Phys. Chem.* **93,** 5953–5957.
23. Kirmaier, C. & Holten, D. (1990) *Proc. Natl. Acad. Sci. USA* **87,** 3552–3556.
24. Fleming, G. R., Martin, J. L. & Breton, J. (1988) *Nature (London)* **333,** 190–192.
25. Kirmaier, C., Holten, D. & Parson, W. W. (1985) *Biochim. Biophys. Acta* **810,** 49–61.
26. Parson, W. W., Nagarajan, V., Gaul, D., Schenck, C., Chu, Z.-T. & Warshel, A. (1990) in *Photosynthetic Bacterial Reaction Centers*, ed. Michel-Beyerle, M. E. (Plenum, New York), in press.
27. Jortner, J. (1980) *J. Am. Chem. Soc.* **102,** 6676–6686.
28. Warshel, A., Chu, Z.-T. & Parson, W. W. (1989) *Science* **246,** 112–116.
29. Marcus, R. A. & Sutin, N. (1985) *Biochim. Biophys. Acta* **811,** 265–322.
30. Bixon, M. & Jortner, J. (1989) *Chem. Phys. Lett.* **159,** 17–20.
31. Marcus, R. (1988) *Chem. Phys. Lett.* **146,** 13–22.
32. Bixon, M., Jortner, J., Plato, M. & Michel-Beyerle, M. E. (1988) in *The Photosynthetic Bacterial Reaction Center*, eds. Breton, J. & Vermeglio, A. (Plenum, New York), pp. 399–419.
33. Warshel, A., Creighton, S. & Parson, W. W. (1988) *J. Phys. Chem.* **92,** 2696–2701.
34. Becker, M., Nagarajan, V., Middendorf, D., Shield, M. A. & Parson, W. W. (1990) *Current Research in Photosynthesis*, ed. Baltscheffsky, M. (Kluyver, Dordrecht, F.R.G.), Vol. 1, pp. 101–104.